

**Modelling, Identification and Control of A  
"Magnetic Levitation CE152"**

Eng. Khalid Abdelhafiz Ali\*

Prof. Mohammed Abdelati\*\*

Assoc. Prof. Mohammed Hussein\*\*\*

**المخلص**

عمل مودل محاكاة "جهاز التعليق المغناطيسي CE152"  
وتعريف قيم متغيراته والتحكم به

CE152

( )

**ABSTRACT**

**Modelling, Identification and Control of A  
"Magnetic Levitation CE152"**

This project takes a comprehensive look at model development for a laboratory magnetic levitation with the final aim to design a control system is presented. The **CE152** made by Humusoft is a laboratory magnetic levitation system designed for studying system dynamics and control engineering principles. First, the magnetic levitation system set-up is depicted, then the whole system is disassembled into simpler subsystems, then theoretical modelling is systematically described. Identification of the necessary parameters is tackled using direct and indirect measurement methods and their results are presented. As the system is nonlinear and

\* Technical Instructor at Gaza Training College (UNRWA, GTC).

\*\* Electrical Engineering Department Head at Islamic University of Gaza (IUG).

\*\*\* Associate Dean of Engineering for Research & Development at Islamic University of Gaza (IUG)

## **Modelling, Identification and Control of...**

unstable, it should be linearized at optional operating point and a digital PID controller with a fine tuned parameters is designed to track a small varying input signals. Finally the simulation's model is validated with the real system, the results show the simulation's model is adequately represents the real magnetic levitation system.

**Keywords:** magnetic levitation system, modelling, identification, discrete, real time toolbox, PID, validation.

### **1. Introduction**

Magnetic levitation systems which can suspend objects without any contact attract increasingly attention as means of eliminating Coulomb friction due to mechanical contact. This technology has been widely utilized for various industrial purpose, such as suspension vehicles, suspension bearing, flywheels, magnetic vibration isolation, magnetically suspended wind tunnel, etc (Kim I. and Kim K.,1992) and (O' Connor,1993). Furthermore, in recent years, the need for high performance, accurate magnetic levitation systems is becoming more important.

Modeling is used for analysis, prediction, control and supervision of a system. Models are classified into two types, linear and nonlinear. Most of physical systems are nonlinear as the magnetic levitation model.

System identification is identified as building a mathematical models based on observed data from the dynamical response of a system. The identification process also could be classified into parametric and nonparametric methods:

In the parametric method, the system equation is described by ordinary differential equation (ODE) and difference equation along with a set of parameters, but in the nonparametric: the system doesn't employ a parameter vector in search for a best description, like frequency analysis and a step response.

Moreover, identification means the determination of the model of a dynamic system from input/output measurements. The knowledge of the model is necessary for the design and implementation of a high performance control system.

System identification is an experimental approach for determining the dynamic model of a system. It includes four steps:

- Input/output data acquisition under an experimental setup.
- Finding a suitable model.
- Estimating of the model parameters by comparing the experimental with the simulated data.

- Validation of the identified model. (Loan D. Landau and Gianluca Zito, 2006).

Linear control is a process of closed loop feedback using a linear controller like P, PI, PD or PID. However, by linear control, we can only control the magnetic levitation in a small range and it may be difficult to design a controller which gives satisfactory, anti-disturbing and robustness. Using PID controller, to get good performance is not easy since PID parameters are hard to be determined, root locus technique is used to determine the PID parameters.

Modeling techniques and designing different type of controllers were presented in many literacy, here is a survey of some of the literacy in recent years, an improved model identification method for magnetic suspension system to establish reliable and exact parameters to describe the dynamic motion characteristic. The parameter for each test sample can be calculated under the specific operation conditions after some magnetic field measurements. The results lead effectively to controller design for magnetic suspension system (Lin et al, 1992). A detailed model of the magnetic suspension system which takes into account the nonlinear characteristic of sensor, which measures the position of the sphere, and the electromagnetic inductor is described (Velasco-Villa et al, 2001). The dynamic of suspension system by using the Euler-Lagranges formulation is developed (Yu et al, 2002). A design of an undergraduate course in Active Magnetic levitation which focused on a project where the students modeled, analyzed, simulated, designed and implemented, an active magnetic levitation control system (Watkins John M. and Piper George E., 2003). The Feedback Inc. model 33-210 laboratory scale one DOF magnetic suspension system as an example of a mechatronic sensing and control plant in a DSP control application. The nonlinear mathematical model of the magnetic suspension system was linearized about a desired equilibrium position of  $20.395e - 3$  meters, and the resulting linear mathematical model was used to design classical and optimal state feedback digital controllers for stabilization and tracking is presented (Anakawa et al, 2005). The modeling of the sensor and actuator characteristics of a magnetic levitation system, using two methods: look up table and segmented linear approximation is considered (Yang et al, 2007).

The paper presents a detailed procedure of modeling an exact model for magnetic levitation apparatus (CE152) and designing a PID controller depending on the derived model, this apparatus is one of most important one in the control's laboratory of Islamic University of Gaza. A platform for the system is setup and all material are collected, we hope that our work and

## Modelling, Identification and Control of...

results will help other researchers and students to build on and design different type of models and controllers.

## 2. The Magnetic Levitation and Setup and Structure

Figure 1 shows photo of the magnetic levitation CE152, where the system could be connected to PC IBM compatible computer. The scheme in Figure 2 shows the model interface, it can be considered at two different levels:

- Physical level - input and output voltage to the coil power amplifier and from the ball position sensor.
- Logical level - voltage converted by the data acquisition card and scaled to  $\pm 1$  Machine Unit [MU].

The core part of the model is a steel ball hanging in the magnetic field of the coil. The position of the ball is measured with a magnetic inductive position sensor. The current for the coil is amplified by an external amplifier and therefore is directly proportional to the input voltage. The model is connected to the PC via universal Data Acquisition Card (DAQ), like the HUMUSOFT MF614. Note that all the experiments used in this thesis are done in Matlab-Simulink environment using Real Time Toolbox (Humusoft Company, 2002).

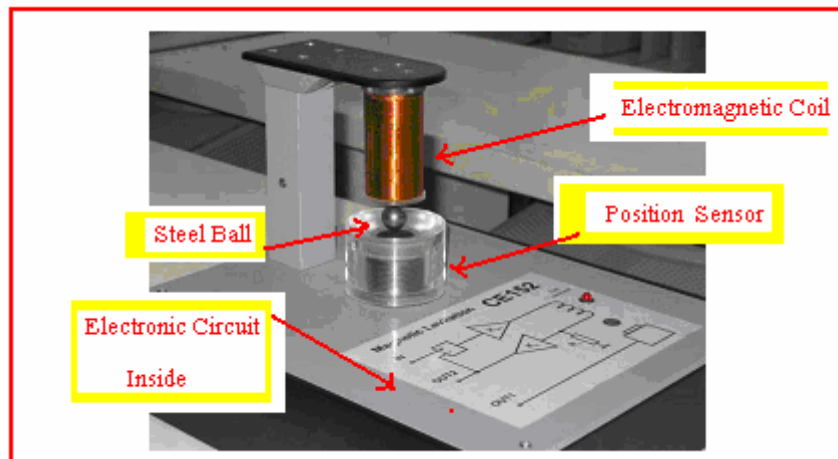


**Figure 1:** Magnetic Levitation System CE152

Later it will be shown that the Magnetic Levitation Model can be approximated by a single input single output nonlinear dynamic system of order 2 or 3 depending on the modeling precision.

The complete system is shown in Figure 2 consists from the following blocks:

- D/A Converter

- The Power Amplifier
- Electromagnetic Force Model
- The Position Sensor
- A/D Converter

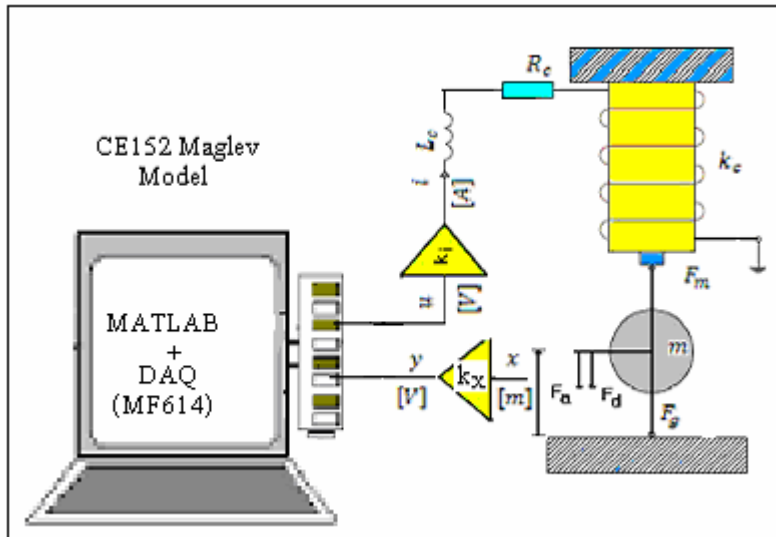


**Figure 2:** Scheme of the Magnetic Levitation System CE152. We will model each block separately, beginning with D/A converter block, and ending with A/D Converter block.

### 2.1 D/A converter

The DAQ card MF614 has four single-ended output channels with resolution 12-bit, and input voltage ranges  $\pm 10v$ . The D/A converter can be represented by a Simulink block; it is shown in Figure 3 and described by a linear function (conversion time very short) given in Equation 1.

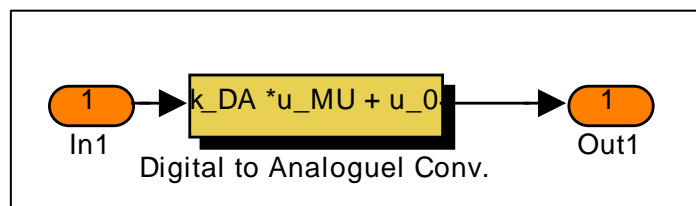


**Figure 3:** Digital to Analog Converter model.

$$u = k_{DA} u_{MU} + u_0 \quad (1)$$

where:

## Modelling, Identification and Control of...

$u$	= Model Output Voltage	[V]
$u_{MU}$	= D/A Converter Input	[MU]
$k_{DA}$	= D/A Converter Gain	[V/MU]
$u_0$	= D/A Converter Offset	[V]

### 2.2 The Power Amplifier

The power amplifier is designed as a source of constant current with the feedback current stabilization. The power amplifier internal structure is shown in Figure 4. The amplifier and coil subsystem can be modelled with the transfer function of 1st order given in Equation 2, and the power amplifier block is shown in Figure 5,

$$\frac{I(s)}{U(s)} = k_i \frac{1}{T_a s + 1} \quad (2)$$

where:

$$k_i = \frac{k_{am}}{(R_c + R_s) + k_{am} k_s R_s} ; \quad (3)$$

$$T_a = \frac{L_c}{(R_c + R_s) + k_{am} k_s R_s} ; \quad (4)$$

$k_i$  is called coil and amplifier gain and  $T_a$  is called coil and amplifier time constant.

Note: because  $T_a$  is very small as we will show later in section 4.2, so Equation 2 becomes:

$$i = k_i u \quad (5)$$

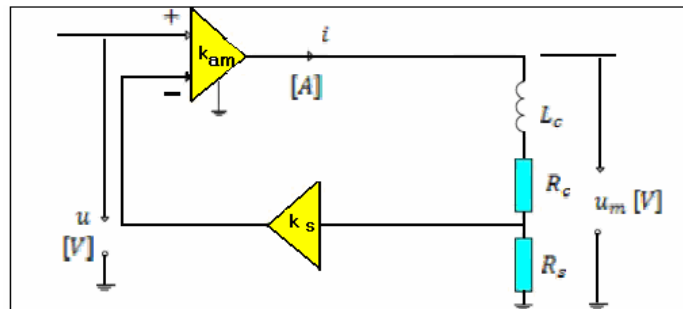


**Figure 4:** The Power Amplifier Internal Structure

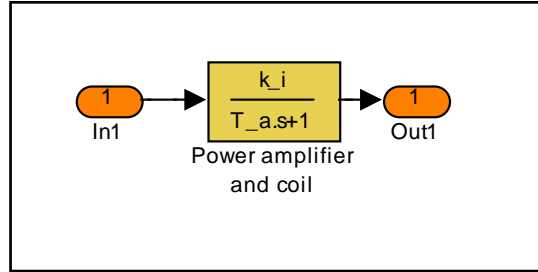


Figure 5: Power Amplifier and Coil Model.

### 2.3 Electromagnetic Force Model

This model can be derived using Lagrange's method, the electromagnetic force is determined from the magnetic co-energy. The derivation of this method is based on the assumptions that the magnetic field distribution is ideal and that the coil inductance varies linearly with suspension distance. An ideal magnetic field distribution is characterized by a uniform field above the suspended object, a magnetic flux density that is a function of distance at fixed current, and a suspended object. The relationship between electromagnetic force, current, and separation distance is assumed to be of general form (Lin and Huei, 1992).

$$F_m = k_c \frac{i^2}{(x-x_0)^2} \quad (6)$$

$$\frac{d}{dt} (m_k \dot{x}) + m_k g = -k_{FV} \dot{x} + k_c \frac{i^2}{(x-x_0)^2}$$

$$m_k \ddot{x} + m_k g = -k_{FV} \dot{x} + k_c \frac{i^2}{(x-x_0)^2} \quad (7)$$

where:

$m_k$	= Ball Mass	[kg]
$F_g$	= Gravity Force	[N]
$F_c$	= Accelaration Force	[N]
$F_d$	= Damping Force	[N]
$x$	= Distance	[m]

### Modelling, Identification and Control of...

$x_0$	= Coil Offset	[m]
$i$	= Coil Current	[A]
$g$	= Gravity Constant	[m/s <sup>2</sup> ]
$k_c$	= Aggregated Coil Const.	[N/A]
$t$	= Time	[s]
$k_{FV}$	= Damping Constant	[N. s/m]

Rearranging Equation 7, the dynamic differential equation of motion becomes;

$$m_k \ddot{x} + k_{FV} \dot{x} = \frac{i^2 k_c}{(x - x_0)^2} - m_k g \quad (8)$$

Note that in some cases the damping force  $F_d$  is very small, for example in case of a low varying tracking signal like a sinusoidal with a very small amplitude and low frequency, but it is large in case of a tracking signal like a square with a high frequency, so the modeling equation will be considered two cases, the first one with damping force which is shown in Equation 8, and second one without damping force which is shown in Equation 9.

$$m_k \ddot{x} = \frac{i^2 k_c}{(x - x_0)^2} - m_k g \quad (9)$$

If we substitute  $i = k_i u$  in Equation 5, we get

$$m_k \ddot{x} = \frac{(k_i u)^2 k_c}{(x - x_0)^2} - m_k g \quad (10)$$

or

$$m_k \ddot{x} = \frac{u^2 k_f}{(x - x_0)^2} - m_k g \quad (11)$$

where:

$$k_f = k_i^2 k_c$$

$k_f$  is called aggregated coil const. [N /V ].

Both Equation 8 and Equation 9 can be represented in Simulink model as shown in Figure 6 and Figure 7 respectively.

### 2.4 Position Sensor

An inductive sensor is used to measure the ball position  $x$ . The position of the ball is obtained by reading the voltage in MU, the voltage varies with ball position, the relationship between ball position and sensor voltage  $y$  is approximately linear and is valid for a height distance range from 0 to 6.3 mm.

To create the relationship between detected voltage  $y$  and ball position, the ball is placed at known positions and then the detected voltages are recorded. Two known positions are measured and plotted as shown in Figure 13, the ball position equation is in the form of Equation 12 and a Simulink block shown in Figure 8.

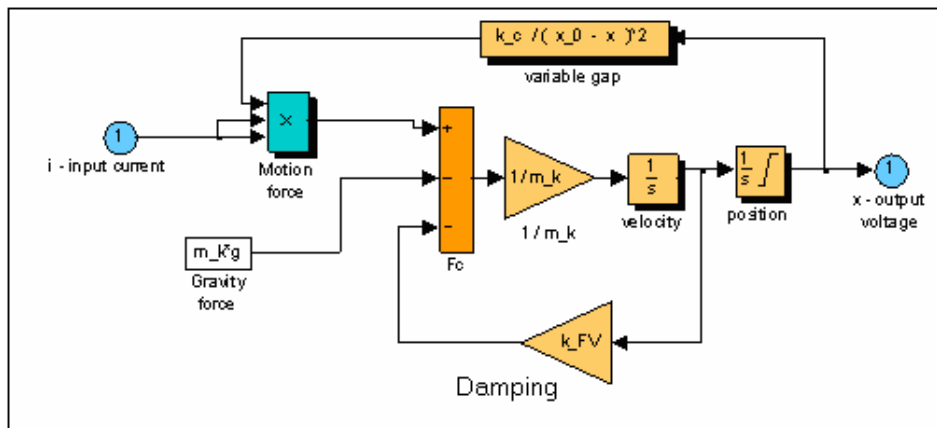
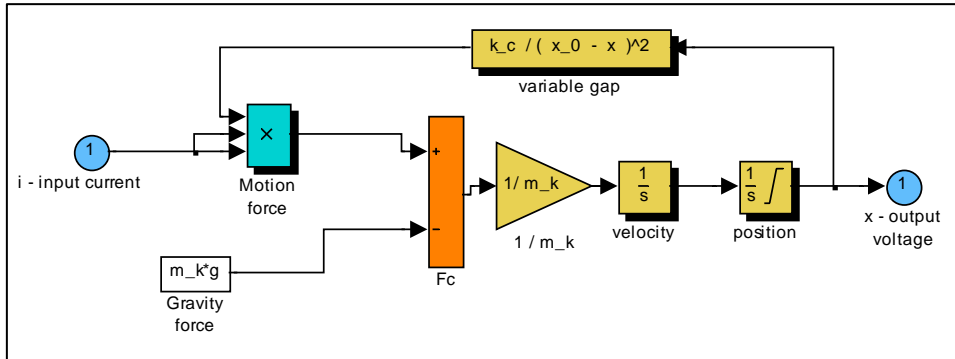
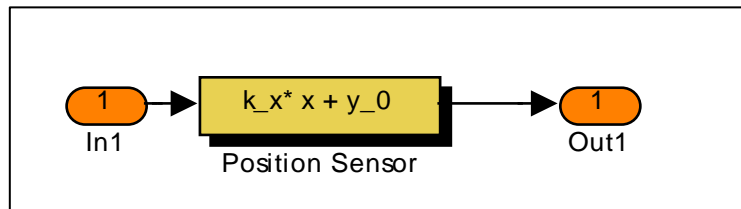


Figure 6: The Ball and Coil Subsystem Model (damping force included).

## Modelling, Identification and Control of...



**Figure 7:** The Ball and Coil Subsystem Model (damping force excluded).



**Figure 8:** Position Sensor Model.

$$y = k_x x + y_0 \quad (12)$$

where:

$k_x$	= Position Sensor Gain	[V/MU]
$y_0$	= Position Sensor Offset	[m]
$x$	= Ball Position	[m]
$y$	= Sensor Output Voltage	[V]

### 2.5 A/D converter

The DAQ card MF614 has also eight single-ended input channels with programmable gain, resolution 12-bit, conversion time  $10\mu\text{s}$ , and input voltage ranges ( $\pm 10\text{v}$ ,  $\pm 5\text{v}$ ,  $0-10\text{v}$ ,  $0-5\text{v}$ ). The A/D converter can be represented by a Simulink block, it is shown in Figure 9, and is described by a linear function (conversion time very short) given in Equation 13.

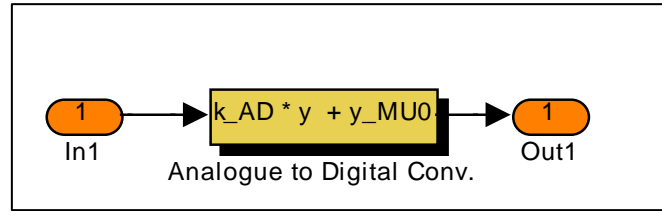


**Figure 9:** Analog to Digital Model.

$$y_{MU} = k_{AD} y + y_{MU0} \quad (13)$$

where:

$y_{MU}$  = A/D Converter Output [V]

$k_{AD}$  = A/D Converter Gain [MU/V]

$y_{MU0}$  = Converter Offset [MU]

$y$  = Model Output Voltage [V]

Using Equation 1 to Equation 13, a Simulink block diagram of the whole system is developed and arranged in Figure 10.

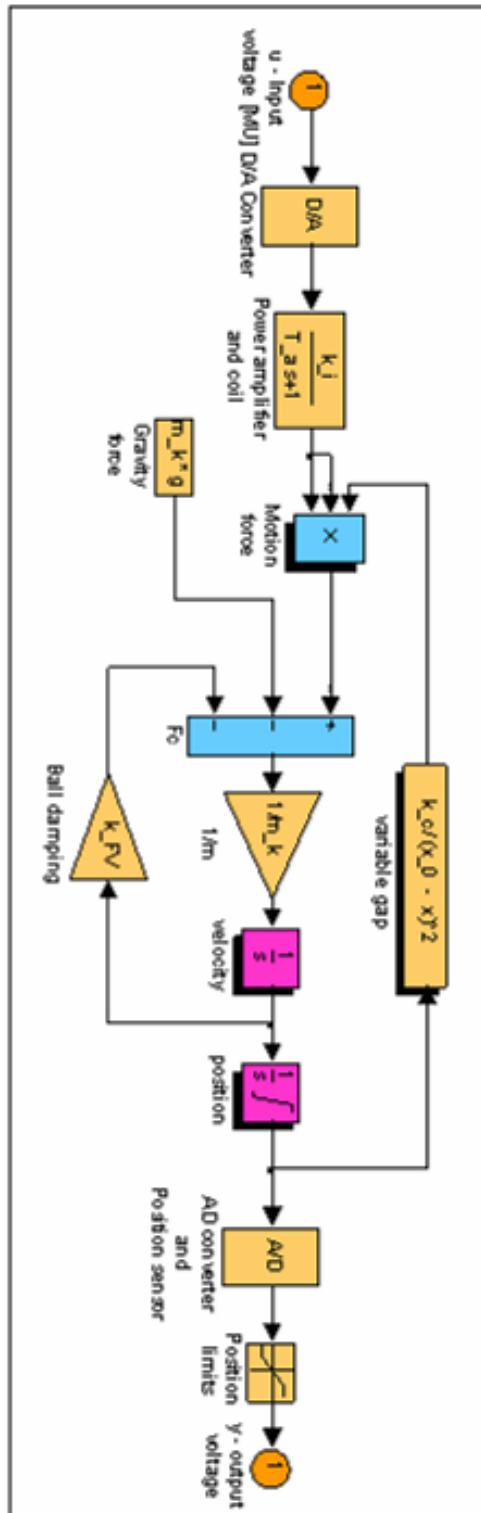


Figure 10: The Whole System Model.

### 3. Measurements and Identification of the Parameters

Once the theoretical model of the laboratory magnetic levitation set-up is obtained, then a thirteen (13) parameters have to be determined:  $k_c$ ,  $k_f$ ,  $x_0$ ,  $m_k$ ,  $y_{MU0}$ ,  $k_{AD}$ ,  $u_0$ ,  $k_{DA}$ ,  $k_x$ ,  $y_0$ ,  $k_{FV}$ ,  $T_a$ , and  $k_i$ , there are two possible approaches:

- Direct measurements of the accessible physical quantities;
- Identification, i.e. experimental estimation of the parameters by means of measuring inputs and outputs.

#### 3.1 Parameters of A/D and D/A Converters

In order to identify the A/D converter parameters, a simple experiment is implemented, we apply a different voltage values at the input of A/D channel and read the corresponding values at the computer side, and fill in Table 1.

**Table 1: Data at Input Channel of DAQ**

$i$	$y[V]$	$y_{MU}$
1	5	1
2	-5	-1
3	0	0

In order to identify the D/A converter parameters, a simple experiment is implemented, we apply a different values in Machine Unit (MU) and measure the output voltage at the outside of DAQ, and fill in Table 2.

**Table 2: Data at Output Channel of DAQ**

$i$	$u_{MU}$	$u [V]$
1	1	5
2	-1	-5
3	0	0

Based on the measurement in Table 1 and Table 2, the following parameter values are obtained:

$$\begin{aligned}
 k_{DA} &= 5 [V / MU] \\
 u_0 &= 0 [V] \\
 k_{AD} &= 0.2 [MU / V] \\
 y_{MU0} &= 0 [MU]
 \end{aligned}$$

## Modelling, Identification and Control of...

**Note:** we used Data Acquisition card from Humusoft **MF614**, and during the experiment above, the DAQ is software selected at  $\pm 5$  volts.

### 3.2 The Power Amplifier

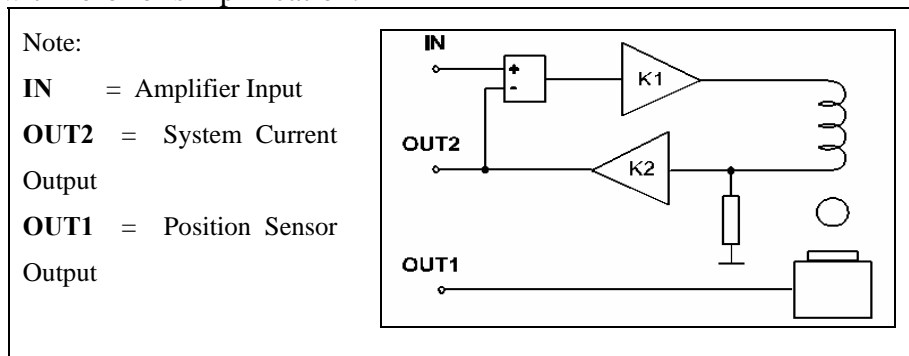
In case that the typical values of the discrete electronics components of the power amplifier are available, we can use them to identify the power amplifier transfer function parameters  $T_a$  and  $k_i$  by directly substituting in Equation 3 and Equation 4. Otherwise, use experimental identification method, applying input signal like a square function at the input of the block (IN) and record the output signal of the block (OUT2), see the base unit diagram of the apparatus Figure 11.

Figure 12 shows the experimental results, where  $k_i$  and  $T_a$  can be determined,

$$k_i = 0.3 [A / V ]$$

$$T_a = 0.3 \times 10^{-3} [s].$$

Note that the time constant is very small so it can be neglected by replacing it with zero for simplification.



**Figure 11:** Base unit diagram of the Magnetic Levitation Model (CE152)

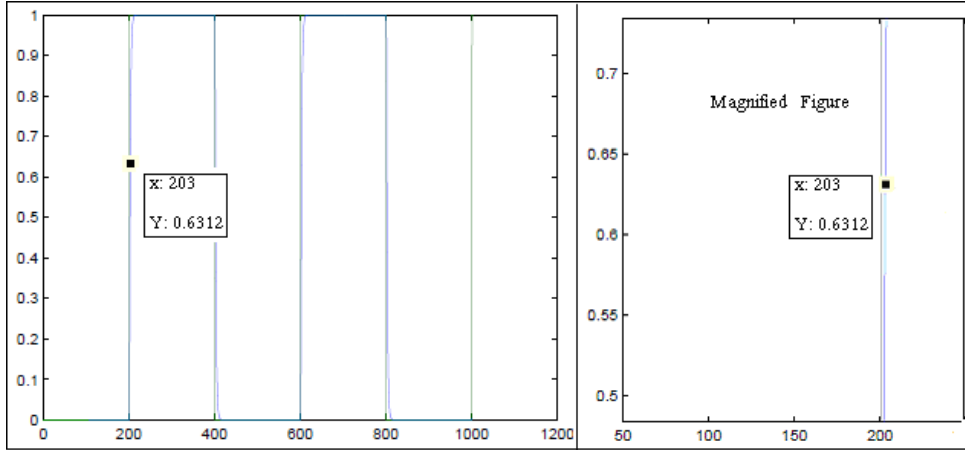


Figure 12: The step response of the power amplifier block (on the right magnified one)

### 3.3 The Position Sensor

The position sensor can be calibrated by simple ball position measurements as shown in Table 3, note that  $k_{AD}=5$  is set for measurements in table 3, and the calibration curve is plotted in Figure 13.

Table 3: Data for Position Sensor Calibration

$i$	$y_{MU}$	$y_i$	$x_i$
1	0.0025	0.0125	0
2	0.774	3.87	$6.3 \cdot 10^{-3}$

The position sensor parameters can be calculated as follows,

$$k_x = (y_2 - y_1) / (x_2 - x_1)$$

$$y_0 = y_1 = 0.0125$$

$$k_x = 612.3016 \text{ [V / m]}$$

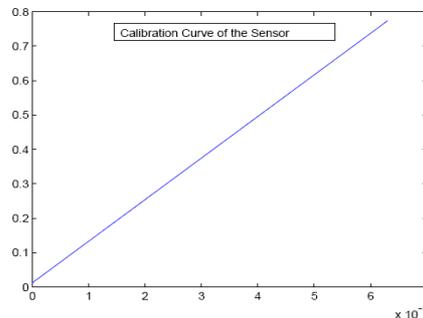


Figure 13: Ball Position vs. Detected voltage in MU

## Modelling, Identification and Control of...

### 3.4 Electromagnetic Force Model

#### 3.4.1 Ball Mass

The mass of the ball is measured by using a precision balance and it is approximated numerical value:

$$m_k = 8.4 \times 10^{-3} [\text{kg}].$$

#### 3.4.2 Coil Constant

The coil constant parameters  $k_f$  and  $x_0$  are estimated by means of interpolation technique, two interpolation techniques are used to calculate the coil constant parameters, firstly we used the *Two Point* interpolation method then the *Linear Quadratic (LQ)* Optimal method, then we compare between them to choose the best one according to the least square error or the minimum cost function.

##### ❖ Two Points Interpolation Method

In Figure 14, we processed the data using **Two Point** interpolation method, the sample data was 4 points of the system input voltage versus the ball position, by plotting  $u$  versus  $x$ , and interpolate the data, see the upper left plot in Figure 14. By equating the magnetic force at a number of different points at points  $x_2$  and  $x_3$  for example, we can find  $x_0$  using the equation below:

$$x_0 = \frac{\frac{x_3 - x_2}{u_3 - u_2}}{\frac{u_3}{u_3} - \frac{u_2}{u_2}}$$

By substituting with numerical values, we get  $x_0 = 0.0095$  [m] .

To find  $k_f$ , we equate the magnetic force to the weight of the ball at equilibrium point,

$$m_k g = \frac{u^2 k_f}{(x - x_0)^2}$$

Then:

$$k_f = m_k g \frac{(x_2 - x_0)^2}{u_2^2}$$

By substituting with numerical values, we get  $k_f = 0.71214 \times 10^{-6}$ , and  $k_c = k_f / k_i^2 = 7.9126 \times 10^{-6}$ .

### ❖ LQ Optimal Method

We processed the data using *Optimal Linear Quadratic* method to fit the parameters in an optimal way. This criterion of optimality is a minimization of the sum of squared errors of estimated equilibrium force (Landau and Zito, 2006: 247) see Equation 14, the sample data is obtained with closed loop control and applying a low and slowly varying sinusoidal tracking signal. The sample data was a large number of data points of the system input voltage  $u(k)$  versus the ball's position  $x(k)$ , these sampled two signals  $x(k)$  and  $u(k)$  are shown in Figure 14 (plot at upper right),

$$J = \sum_i \left( \frac{u_i^2 k_f}{(x - x_0)^2} - m_k g \right)^2 \quad (14)$$

using a minimization procedure of the least square error to calculate the constant  $x_0$  and then calculating the constant  $k_f$ .

The Coil Constant Parameters are;

$$x_0 = .0083 \text{ [m]}$$

$$k_f = .609 \cdot 10^{-6} \text{ [N / V]}$$

$$k_c = 6.9 \times 10^{-6} \text{ [N / A]}$$

### ❖ Comparison of the Two Interpolation Methods

To compare the error in the two methods, one should calculate the error by plotting the magnetic force  $F_m$  in time domain in each method, and then you can compare, see plot of  $F_m$  at lower left in Figure 14 for the first method (Two Point method) and plot for  $F_m$  at lower right in Figure 14 for the second method (LQ method).

Of course that the error generated by LQ method is smaller than that generated by Two Point method, so the parameter values of the second method (LQ) will be considered.

#### 3.4.3 Damping Constant

For more accurate and exact model, the ball damping constant  $k_{FV}$  should be estimated using offline model adaptation, by comparing the real response  $y_{real}$  with the model response  $y_{mod}$  using *Parameter Estimation Toolbox* through optimization algorithm like Simplex Search, In this technique the Simulink model is tuned until the Simulink model matched the real time model to a Least Square Error Cost Function (LSECF). After much iteration, the following satisfied result is obtained.

## Modelling, Identification and Control of...

$$k_{FV} = 0.03$$

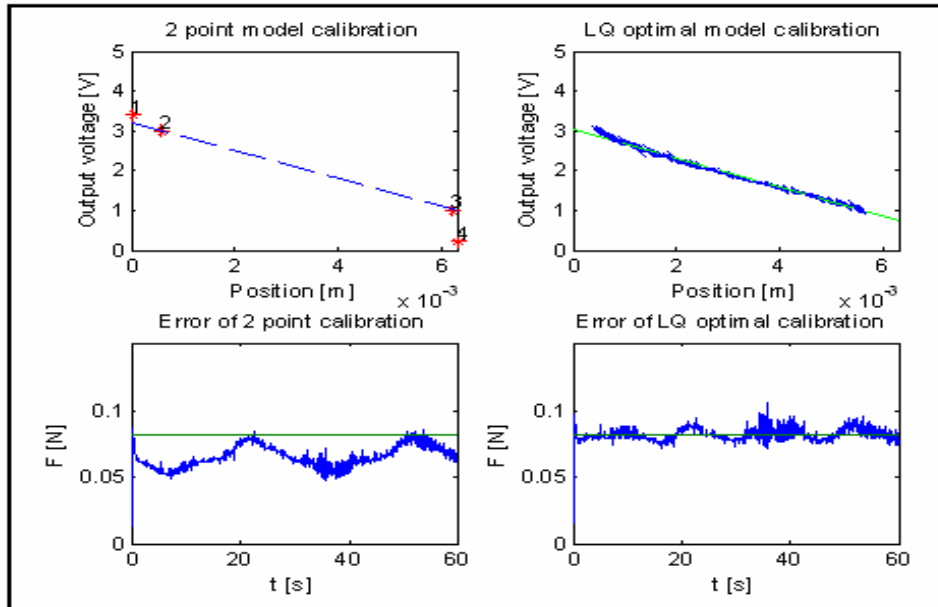


Figure 14: Plots generated during estimation of Coil constant

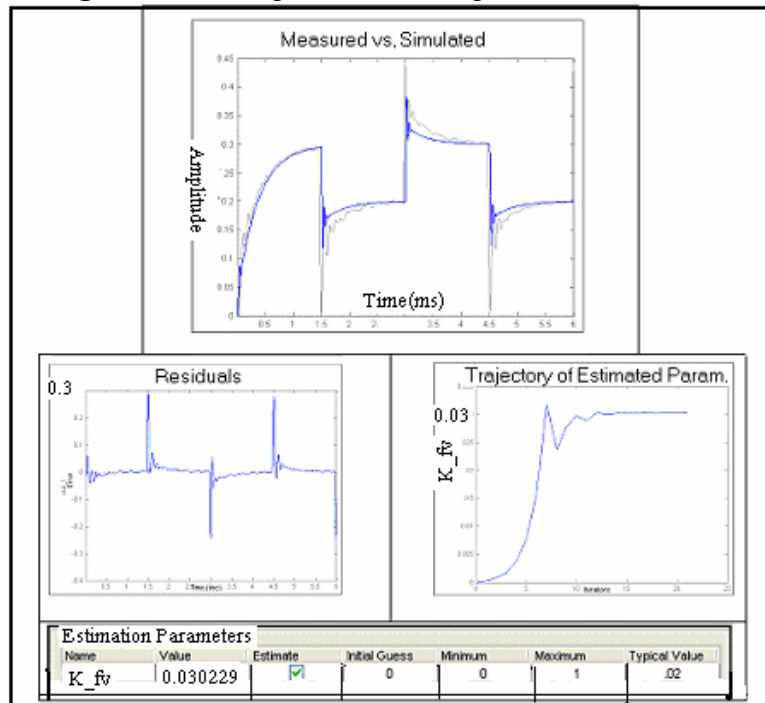


Figure 15: Plots generated during estimation of the damping constant.

Note: In Figure 15, groups of plots are included to show the process of parameter estimation and to justify the result.

#### 4. CONTROLLER DESIGN

The governing equations of motion for magnetic levitation (maglev) system are Equations 2, 8, and 12. When the state variables  $x_1 = x$ ,  $x_2 = dx/dt$ ,  $x_3 = i$ , and  $u(t) = u_m$  are introduced, the state-space model of the system becomes

$$\begin{aligned} \dot{x} &= v \\ \dot{v} &= -\frac{k_{FV}}{m_k} v - g + \frac{k_c i^2}{m_k (x_0 - x)^2} \\ \dot{i} &= \frac{k_i k_{DA} u_m}{T_a} - \frac{i}{T_a} \\ y_m &= k_x k_{AD} x \end{aligned} \quad (15)$$

where  $x$  is the ball position,  $i$  is the coil current,  $u_m$  is the model input voltage and  $y_m$  is the A/D converter output. This model is nonlinear, but an approximation can be made which linearizes the system about a set of operating position. This linearization is only valid for a limited range of operation, and the linear model may contain time varying elements. The method used to linearizes this system expands the nonlinear state equation into a Taylor series about a nominal point usually the equilibrium point, the equilibrium point for this system is  $[x_{00}, v_{00}, i_{00}]$ . All the terms of the Taylor series of order higher than the first are discarded.

$$\begin{aligned} \dot{x}_\delta &= v_\delta \\ \dot{v}_\delta &= \frac{-2 i_{00}^2 k_c}{(x_{00} - x_0)^3 m_k} x_\delta - \frac{k_{FV}}{m_k} v_\delta + \frac{2 i_{00} k_c}{(x_{00} - x)^2 m_k} i_\delta \\ \dot{i}_\delta &= \frac{k_i k_{DA} u_\delta}{T_a} - \frac{i_\delta}{T_a} \\ y_m &= k_x k_{AD} x_\delta \end{aligned} \quad (16)$$

Which can be represented in a state space representations as shown below (as  $A$ ,  $B$ ,  $C$  and  $D$  matrices represent the actual state system matrices),

$$\begin{aligned} \frac{dx}{dt} &= Ax(t) + Bu(t) \\ y(t) &= Cx(t) \end{aligned}$$

Where:

### Modelling, Identification and Control of...

$$\mathbf{A} = \begin{bmatrix} 0 & 1 & 0 \\ \frac{-2i_{00}^2 k_c}{(x_{00} - x_0)^3 m_k} & -\frac{k_{FV}}{m_k} & \frac{2i_{00} k_c}{(x_{00} - x)^2 m_k} \\ 0 & 0 & -\frac{1}{T_a} \end{bmatrix}$$

$$\mathbf{B} = \begin{bmatrix} 0 \\ 0 \\ \frac{k_i k_{DA}}{T_a} \end{bmatrix}$$

$$\mathbf{C} = [k_x k_{AD} \quad 0 \quad 0]$$

$$\mathbf{D} = [0] \quad (17)$$

When the parameters of system, and the optional equilibrium point [0.0032 0.0 0.5612] are inserted, then the system's matrices values become as follows,

$$\mathbf{A} = \begin{bmatrix} 0 & 1 & 0 \\ 3834.4 & -2.4 & 35.2 \\ 0 & 0 & -333.3 \end{bmatrix},$$

$$\mathbf{B} = \begin{bmatrix} 0 \\ 0 \\ 500 \end{bmatrix},$$

$$\mathbf{C} = [122.4 \quad 0 \quad 0],$$

$$\mathbf{D} = [0] \quad (18)$$

Note that the equilibrium distance point  $x_{00}$  is chosen approximately in the middle of the space between the magnetic core and the head of the inductive sensor and accordingly  $v_{00}$  and  $i_{00}$  were found ( see the photo in Figure 1).

#### 4.1 Continuous Time Controller Design

Before we can design a controller to stabilize the system, the poles and zeroes of  $H(s)$  should be located. The system transfer function  $H(s)$  of the actual position to the desired position in Equation 19 is obtained from the space state representation in Equation 18.

$$H(s) = \frac{w(s)}{y(s)} = \frac{2.154487 \times 10^6}{(s - 60.73)(s + 63.12)(s + 333.3)} \quad (19)$$

#### 4.2 Analog PID Controller

To design a standard analog **PID** controller for the system with  $H(s)$  given by Equation 19, we should guess the two zeros of the PID controller, see Equation 20.

$$\begin{aligned} H_c(s) &= K_p + \frac{K_i}{s} + K_d s \\ &= \frac{K_d s^2 + K_p s + K_i}{s} \\ &= K_p \frac{(K_d/K_p) s^2 + s + (K_i/K_p)}{s} \\ &= K \frac{K'_d s^2 + s + K'_i}{s} \\ &\text{where } K'_d = K_d/K_p \text{ and } K'_i = K_i/K_p \\ &= K \frac{(T_{zr1} s + 1)(T_{zr2} s + 1)}{s} \end{aligned} \quad (20)$$

#### 4.3 Design and Tuning of PID Controller

Investigating the root locus of the open loop of the magnetic levitation system  $H(s)$  in Figure 16, we can guess the two zeros of the PID controller, after a number of trials, we get a satisfactory trajectory which assigns the two zeros at -200 and -1.5, then the PID controller has Equation 21.

### Modelling, Identification and Control of...

$$H_c(s) = \frac{(s + 200)(s + 1.5)}{s} \quad (21)$$

$$H_c(s) = \frac{s^2 + 201.5s + 300}{s} \quad (22)$$

Normalizing  $K_p$  which is the factor of  $s$  term in Equation 22, Then we can write,

$$H_c(s)H(s) = \frac{(0.005s^2 + s + 1.4888)}{s} \frac{2.154487 \times 10^6}{(s - 60.73)(s + 63.12)(s + 333.3)}$$

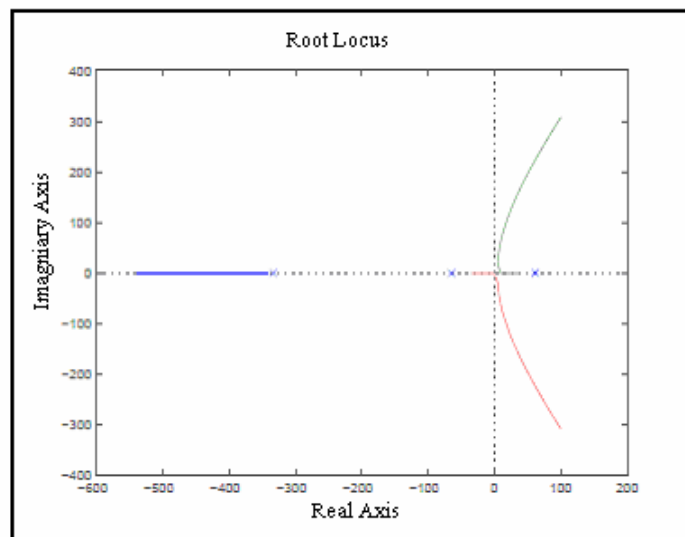


**Figure 16:** A root locus of open loop system  $H(s)$

Now plot the root locus of the open loop of  $H_c(s)H(s)$  and tune controller gain  $K$ , that to move the unstable pole as far to the left as possible, also taking on account a trade-off between minimum overshoot, reasonable control action, and fast transient response. For every  $K$  possible on the root locus trajectory, we tried a number of step response until we have a good system performance see Figure 17, then pick  $K$  which satisfies most of the requirements,  $K$  has a value of **2**. Thus the PID controller parameters are:

$$K_p = 2,$$

$$K_d = K_p K'_d = 0.005 \times 2 = 0.01,$$

$$K_i = K_p K'_i = 2 \times 1.4888 = 2.97$$

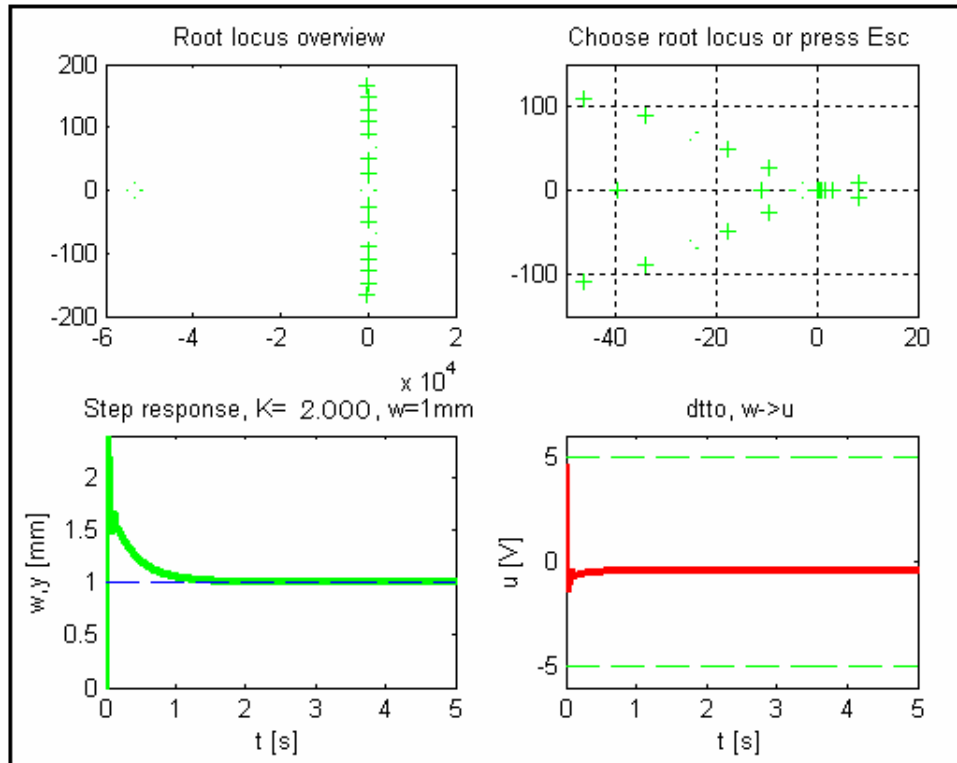


**Figure 17:** Root locus and step response of the system

#### 4.5 Discrete PID Controller

Now we will discretized the standard analog PID controller using a Zero Order Hold (ZOH) method by the substitution:

$$s = \frac{z-1}{zT_s} \quad (23)$$

where:  $T_s = \text{sampling period [s]}$

This will give the Z transform of the standard PID as follow:

$$H_c(z) = K_p + K_i \frac{zT_s}{(z-1)} + K_d \frac{(z-1)}{z} \quad (24)$$

## Modelling, Identification and Control of...

$$= \frac{K_p z(z-1) + K_i T_s z^2 + K_d / T_s (z-1)^2}{z(z-1)} \quad (25)$$

### 4.6 Sampling Rate Selection

Selection of sampling rates is an important issue. For economical reasons, sampling rate is kept as low as possible: A lower rate means that there is more time available for control algorithm execution, which can thereby be carried out on slower computers. Digitizing well-behaved analog control systems can heavily affect system response. If sampling frequencies is too low, the systems may even become unstable. According to the Nyquist criterion (Landau and Zito, 2006: 28), the sampling frequency should at least be twice as high as the bandwidth of the error signal. This bandwidth is bounded by the system bandwidth, hence  $\omega_s \geq 2\omega_B$ .

However, in order to guarantee satisfactory response, a factor of 10 to 20 may be required.

In our case  $\omega_B$  can be determined from frequency response of the desired position to the actual position in Figure 18,

$$\omega_s = 20 \omega_B \quad \text{or} \quad f_s = 20 f_B$$

when  $f_B \approx 50 \text{ Hz}$ , then the sampling frequency  $f_s = 1000 \text{ Hz}$ .

Note: The parameters of the Discrete PID were:  $k_p = 2$ ,  $k_i = 2.97$ ,  $k_d = 0.01$ .

The simulated unit step response for the constructed model is shown in Figure 19.

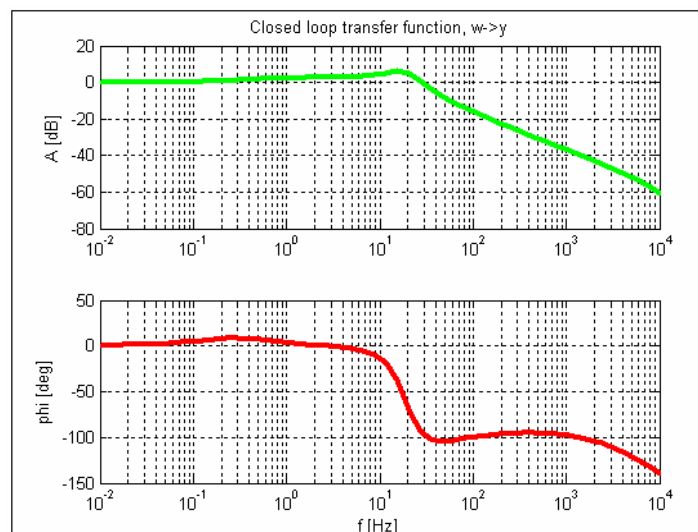
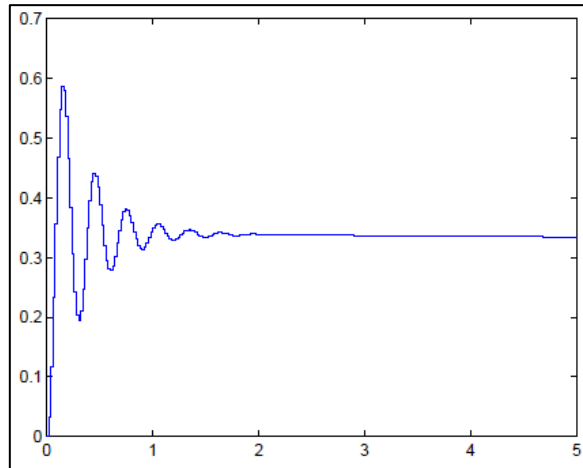


Figure 18: Closed loop transfer function with tuned PID, desired position to actual position.



**Figure 19:** Unit Step Response of the Compensated Discretized System.

## 5. Experimental Results

The validity of the constructed model against the real model should be investigated, therefore a digital controller PID has to be provided, which will enable the tracking of a position reference and the position reference  $w_{ref}$  is a square signal with time period 3s (green line). The comparison between the real response of the position  $w_{real}$  of magnetic levitation model (red line) and of the model (blue line) as shown in Figure 20 shows that the real system response is subject to significant external disturbances. In addition, Figure 21 shows the input signal  $u$  provided by the controllers in case of the real system is the green line and in case of the model is the blue line. From the comparison, we can see that the signals are quite similar in all the recorded period except from (600-900), which occur due to some noise and un-modeled dynamics of the system.

## 6. Conclusions

As a result of this experimental research, a simple control approach was presented, which involves a digital PID controller applied on the linearized model. As modeling and identification of a laboratory magnetic levitation was dealt with, the CE152 laboratory magnetic levitation made by Humosoft presented as a single input a single output. The modeling of magnetic levitation was systematically tackled by disassembling the system into simpler subsystems, i.e. modeling of the sensors, power amplifier dynamics and ball and coil subsystem dynamics. Furthermore, the A/D and

## Modelling, Identification and Control of...

D/A models have been modeled separately. In addition, measurement and identification of all the parameters needed was illustrated. Finally, validation of the developed mathematical model was treated. The validation results with successful experiments suggest that the developed simulation model adequately represents the real laboratory magnetic levitation.

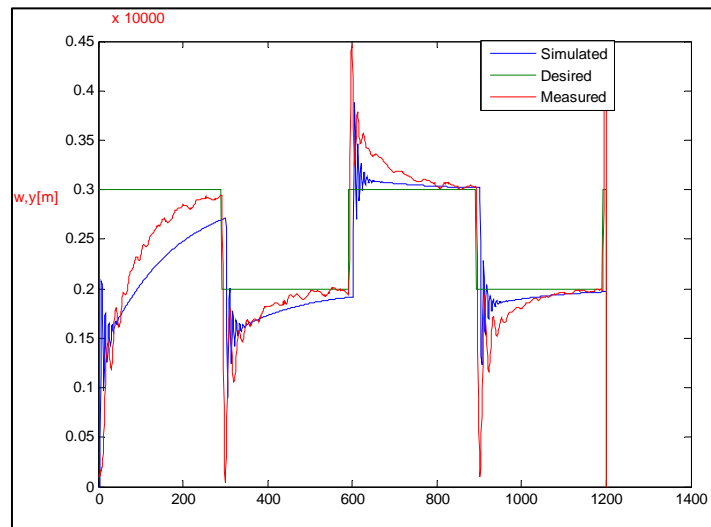


**Figure 20:** Desired, Measured, and Simulated Position.

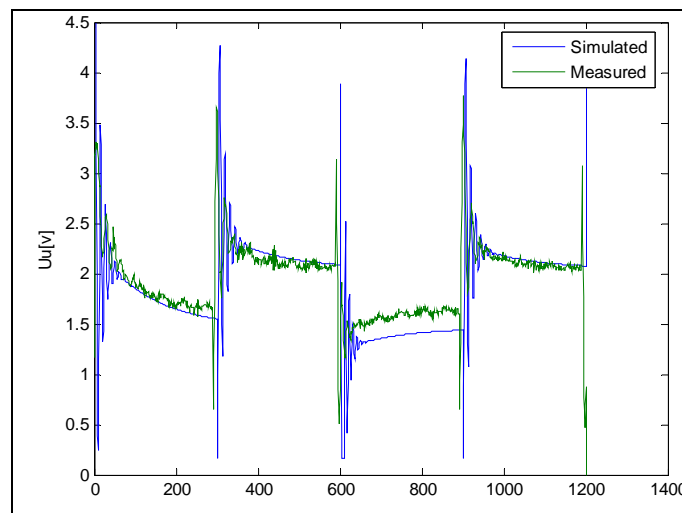


**Figure 21:** Measured and Simulated of controller Output

**References:**

1. Kim, K. I. and K. K Kim 1992: Using Magnetic Suspension in Melting Metals without a Crucible, Soviet Electrical Engineering: 79-88.
2. O' Connor, Leo 1993: U.S. Developers Join Magnetic Rail Push Mechanical Engineering: 75-79.
3. Lin, C.E., H.L Jou, Y.R. Sheu 1992 : Exact Model Identification for Magnetic Suspension System via Magnetic Field Measurement, Institute of Aeronautics and Astronautics, National Cheng Kung University, Taiwan, China.
4. Velasco-Villa, M., Castro-Linares R., Corona-Ramirez L. 2001: Modeling and passivity based control of a magnetic levitation system, Proceedings of the 2001 IEEE International Conference, Vol.3: 64 – 69.
5. H. Yu, T.C. Yang, D. Rigas and B.V. Jayawant, 2002: Modeling and Control of Magnetic Suspension Systems", Proceeding of the 2002 International Conference on Control Applications, Scotland, UK.
6. Watkins J.M., Piper G.E., 2003: An Undergraduate Course in Active Magnetic Levitation: Bridging the Gap", Proceedings of the 35th Southeastern Symposium, pp. 313 - 316, USA, 16-18 March 2003.
7. Ji-Hyuck Yang, Tae-Shin Kim, Su-Yong Shim, Young-Sam Lee, Oh-Kyu Kwon, ``Actuator and sensor modeling for magnetic levitation system", ICCAS 2007, International Conference, pp. 917 - 922, Oct. 2007.
8. Loan D. Landau, Gianluca Zito, 2006: Digital Control Systems - design, identification and implementation, First Edition, Springer Verlag, London.
9. Humusoft 2002: CE 152 Magnetic Levitation Model: User's Manual, Prague.
10. Lin, C. E. and Huei L. Jou, 1992: Force Model Identification for Magnetic Suspension System via Magnetic Field Measurements IEEE Transactions of Instrumentation and Measurement, 767-772.